

# A Novel Class of Strain Gauges Based on Layered Percolative Films of 2D Materials

Marek Hempel,<sup>†</sup> Daniel Nezych,<sup>‡</sup> Jing Kong,<sup>§</sup> and Mario Hofmann<sup>\*,||</sup>

<sup>†</sup>RWTH Aachen University, Aachen, Germany

<sup>‡</sup>Department of Physics, Massachusetts Institute of Technology, Cambridge, Massachusetts, United States

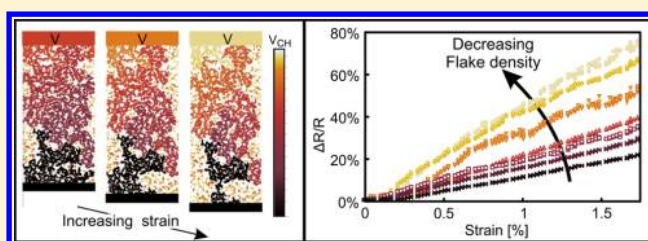
<sup>§</sup>Department of Electrical Engineering and Computer Science, Massachusetts Institute of Technology, Cambridge, Massachusetts, United States

<sup>||</sup>Department of Materials Science and Engineering, National Cheng Kung University, Tainan, Taiwan

## S Supporting Information

**ABSTRACT:** Here we report on the fabrication and characterization of a novel type of strain gauge based on percolative networks of 2D materials. The high sensitivity of the percolative carrier transport to strain induced morphology changes was exploited in strain sensors that can be produced from a wide variety of materials. Highly reliable and sensitive graphene-based thin film strain gauges were produced from solution processed graphene flakes by spray deposition. Control of the gauge sensitivity could be exerted through deposition-induced changes to the film morphology. This exceptional property was explained through modeling of the strain induced changes to the flake–flake overlap for different percolation networks. The ability to directly deposit strain gauges on complex-shaped and transparent surfaces was presented. The demonstrated scalable fabrication, superior sensitivity over conventional sensors, and unique properties of the described strain gauges have the potential to improve existing technology and open up new fields of applications for strain sensors.

**KEYWORDS:** Graphene, strain gauge, gauge factor, percolative transport



Strain gauges are a ubiquitous sensor type that is used in many different applications where the mechanical deformation has to be analyzed, such as structural health monitoring or force sensing. The strain gauge market in 2013 is expected to exceed 4.5 billion USD<sup>1</sup> with major consumers being the oil and gas industry and automotive applications.

A common figure of merit for the sensitivity of the transduction from mechanical to electrical parameters is the gauge factor (GF) that relates the change in electrical resistance to the applied strain, through

$$GF = (\Delta R/R)/\varepsilon$$

where  $\Delta R/R$  is the normalized change in electrical resistance, and  $\varepsilon$  is the mechanical strain.

Conventional strain gauges, relying on geometrical change of conduction path, have gauge factors in the range of 2–5<sup>2,3</sup> and represent a reliable and well-established technology. Other strain gauge types, such as silicon strain gauges, exploit the piezoelectric character of the material and offer gauge factors larger than 100. This type of sensor, however, is more fragile and only designed for little straining. Both types of sensors represent mature technologies which have not witnessed major technological changes in the last decades. Novel applications require higher sensitivity, lower cost, and easier use which has inspired new measurement technologies, such as fiber optic

methods or interferometry. The inability of these new technologies to outperform conventional gauges in all three categories, however, limits their general application. Additionally, potential application areas, such as human motion detectors, force sensitive touch screens, or high resolution deformation analysis, are only accessible with innovative sensors that exhibit stretchability, transparency or can be applied to complex surfaces.

In this work we have developed a novel class of strain gauges that combines cheap and scalable production with high sensitivity and novel, attractive properties. This new gauge type is based on thin films of percolative networks of 2D materials, and the sensing mechanism originates from strain-dependent film morphology changes. This novel sensing mechanism allows the fabrication of strain gauges from a wide variety of materials that do not need to exhibit piezoresistive response and proof of concept devices were fabricated from graphene thin films.

Since its successful isolation in 2004,<sup>4</sup> graphene, a 2-D allotrope of carbon, has attracted great attention due to its unique properties such as extremely high thermal and electrical

**Received:** August 8, 2012

**Revised:** October 4, 2012

**Published:** October 9, 2012

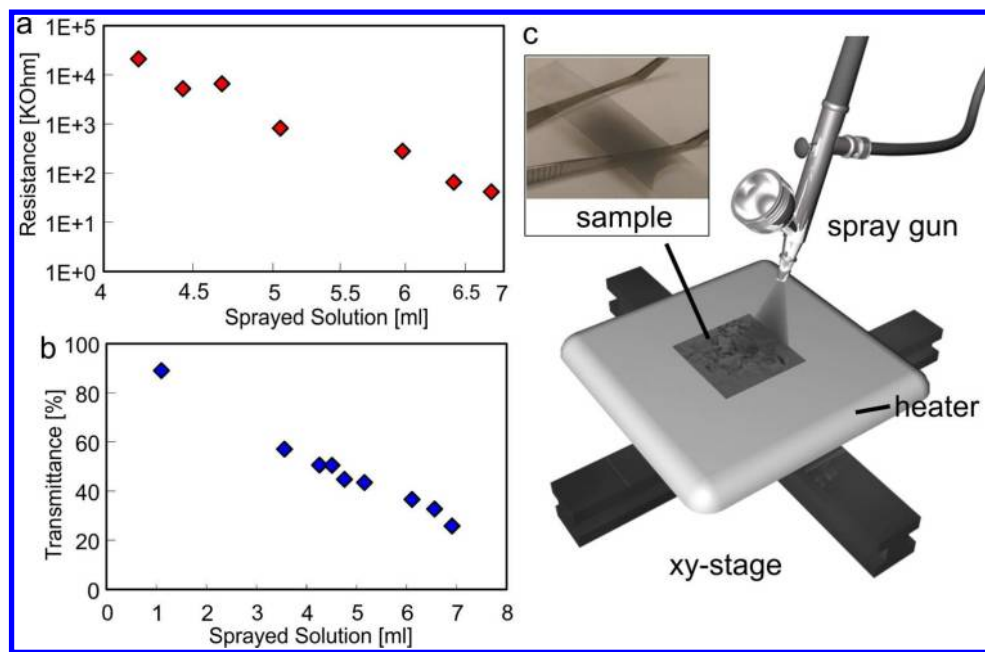


**Figure 1.** Characterization of the spray coating process. (a) Double-logarithmic plot of sample resistance vs amount of sprayed solution. (b) Film transmittance vs amount of sprayed solution. (c) Schematic of experimental setup (inset) as-prepared LPF device.

conductivity<sup>5,6</sup> and mechanical strength. The intense and interdisciplinary work on graphene has led to a variety of applications, in particular in the field of sensors.<sup>7</sup> With respect to strain sensors, different approaches have been examined to compete with conventional strain gauges. Using the piezoresistive properties of graphene, strain sensors with gauge factors of 0.55 and 6.1 have been fabricated.<sup>8,9</sup> Graphene flakes incorporated in a polymer matrix have been suggested for health monitoring.<sup>10</sup> Recently nanographene films have been synthesized whose piezoresistive response can be controlled by changing their growth parameters resulting in GFs of over 300.<sup>11</sup> The gauge factor obtained by these approaches compares favorably with metal strain gauges, but this improvement comes at the cost of higher complexity of manufacturing those carbon based strain gauges compared to metal films.

We here demonstrate the facile and scalable fabrication of graphene-based layered percolative film (LPF) strain gauges that exhibit a high sensitivity. Different from existing strain gauges, this sensitivity can be tuned over a wide range of values by adjusting the deposition parameters. A model to explain this behavior is developed and verified. The described novel device class has several advantages over existing strain gauges, such as compatibility with a wide range of materials, ease of deposition, and novel properties. This work has the potential for improving existing strain gauge technology and open up new fields of application.

**Experimental Section.** Graphene represents an ideal starting material for layered 2D films. Its weak interlayer adhesion permits easy isolation of individual, atomically thin sheets. Percolative networks of graphene layers can be obtained by the assembly of micrometer sized flakes with high enough density so that overlap between neighboring flakes occurs.

Percolative film devices were fabricated on flexible plastic substrates by spray-deposition of a graphene solution. This solution was produced by expansion of commercially available intercalated graphite flakes (Asbury 3772) through microwave irradiation and subsequent mechanical exfoliation by sonication

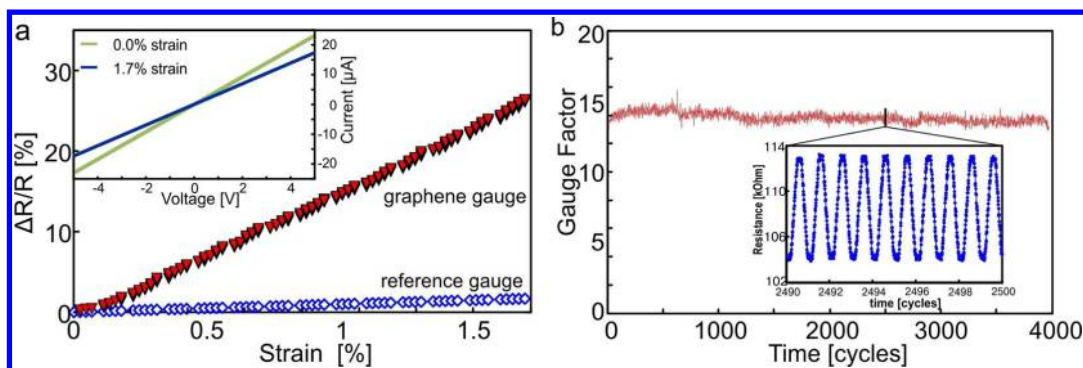
in 1-methylpyrrolidone (NMP) solvent, according to reports by Xin et al.<sup>12</sup> followed by a solvent exchange described by Zhang et al.<sup>13</sup> (The synthesis procedure and analysis of the obtained material are described in detail in the Supporting Information.) The used spray coating process allows the control of the graphene film morphology through the variation of process parameters. Figure 1a shows that the film resistance decreases with the amount of deposited solution as expected since a larger number of conductive pathways is generated as more flakes are overlapping. Consequently, an inverse power law dependence is observed as predicted for percolation systems.<sup>14</sup> The film transmittance, as depicted in Figure 1b, decreases linearly with deposited material volume.

The spray deposition approach offers the ability to produce high quality graphene thin films at large scales, and  $10 \times 20$  mm sample sizes were used in the presented experiments as shown in the inset of Figure 1c. The ability to generate more complex device structures through shadow-masked spray deposition is discussed in the Supporting Information.

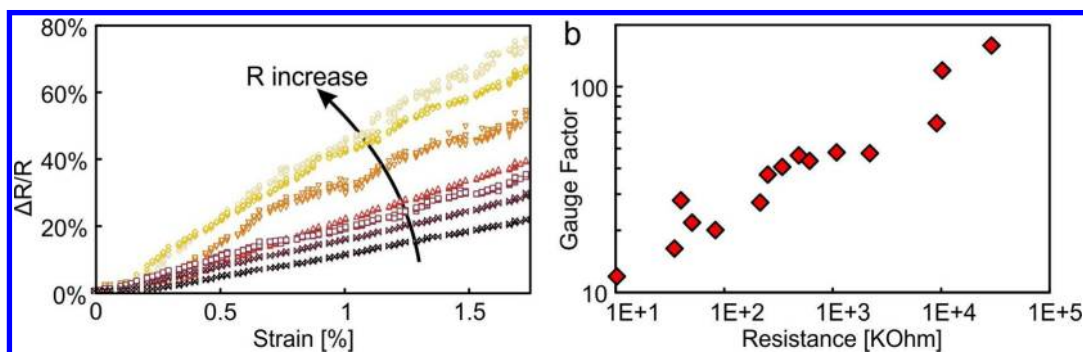
**Results.** The thus-fabricated LPF samples were subjected to uniaxial strain by uniformly bending the graphene coated PET substrates to a defined radius. Since the graphene film thickness on top of the substrate surface is smaller by at least 3 orders of magnitude compared to the substrate thickness (PET thickness  $160 \mu\text{m}$ ), the graphene film can be expected to be uniaxially strained uniformly across its thickness.<sup>15,16</sup>

Figure 2a shows a typical curve of the relative change in resistance  $\Delta R/R$  as a function of mechanical strain  $\epsilon$ . The good linear response of the graphene gauge over a wide range of mechanical strain demonstrates the usefulness of this device structure for strain sensing. The sensitivity of the graphene strain gauge—as indicated by the slopes of  $\Delta R(\epsilon)$ —was found to be significantly larger than commercial metal film strain gauges. As shown in the inset of Figure 2a, the graphene device retains its ohmic behavior during straining.

Reliability tests were carried out to evaluate the long-term stability of the devices. The result of repeated cycling of a strain gauge for 4000 times is shown in Figure 2b.



**Figure 2.** Characterization of graphene film based strain gauge. (a) Plot of normalized change in electrical resistance vs strain for graphene and metallic reference gauge. (inset) Representative current–voltage response with and without applied strain. (b) Reliability measurement of gauge factor over 4000 straining cycles. (inset) Representative plot of resistance for 10 cycles of part b.



**Figure 3.** Relation between gauge factor and resistance from various samples. (a) Curves of normalized change in electrical resistance versus strain for several strain gauges. (b) Extracted gauge factor versus initial resistance for different devices.

The gauge factor remains constant over the measured 4000 cycles with a standard deviation of 2.1 %. The small change of the electrical properties of graphene under cyclic mechanical stress can be explained by the low friction between sliding graphene layers that is exploited in graphite-based solid lubricants.

Depending on the deposition-controlled morphology of the graphene film, the film resistance can vary over several orders of magnitude. To compare strain gauges fabricated from films with different resistances, the change in resistance  $\Delta R$  of a device is normalized to its initial resistance. A set of thus normalized curves of different strain gauges is shown in Figure 3a. The slope of these curves is identical to the gauge factor, and when plotting the extracted gauge factors as a function of initial resistance (Figure 3b) a clear correlation can be seen. The linear dependence in the log–log plot of Figure 3b indicates a power law dependence and hints to a different underlying mechanism than observed by Zhao et al.<sup>11</sup> as detailed subsequently. The observation that high resistivity samples exhibit a larger sensitivity to strain variation offers a route to tune the gauge factor by adjusting the film resistance. For traditional strain gauges that analyze the change in conductance of a homogeneous material (i.e., piezoresistive sensors or metallic gauges), the gauge factor is a constant. The capability of adjusting the gauge factor demonstrated here has several advantages. Gauge factors could be tuned to a specific value to serve as replacements for conventional gauges or they can be adjusted to the needs of individual applications, for example, high GF for low-strain applications and low GF for high deformation applications. Finally, the gauge factor can be optimized to compromise between sensitivity and noise to

produce very accurate low noise sensors with low resistance or high sensitivity sensors at the cost of increased noise.

The observation that the gauge factor is related to the resistance of the graphene film raises the question about the underlying working principle of the strain gauge. Raman spectra taken in unstrained and strained condition reveal that no discernible shift of G-band or G'-band peaks occurs (see Supporting Information). This observation suggests that the graphene flakes are not deforming with the gauge.<sup>16</sup> Instead, to accommodate the extension of the strain gauge, slippage of overlapping graphene flakes occurs. The conductivity between neighboring flakes is determined by their overlap area and the contact resistance. Upon application of strain to the film, the separation between neighboring flakes becomes larger due to slippage, and thus their overlap area decreases. The resulting increase in resistance represents the working principle of our thin film strain gauge. This is a different operation mechanism from traditional strain gauges that rely on the variation of resistance within the strain sensing material.

We analyze this behavior by modeling the percolation of current through a network of randomly positioned circular flakes with a uniform size distribution (Figure 4a). The contact resistance of overlapping flakes is determined by calculating their contact area. The resistance of the whole flake network is then calculated by solving the Kirchhoff equations for a large resistor network of contact resistances and in-flake resistances. The effect of strain is implemented by displacing the flakes according to the elongation of the whole device and recalculating the network resistance. Figure 4a shows that the voltage drop across such a simulated percolating network at a

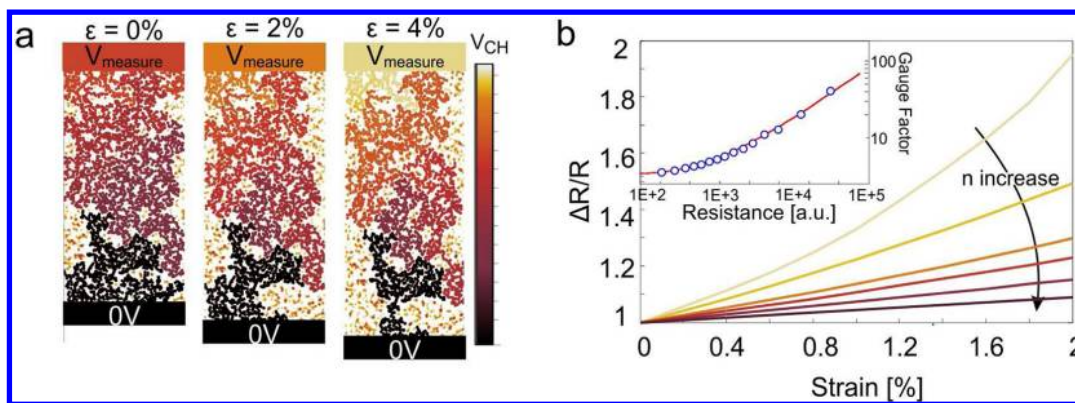


**Figure 4.** Modeling of percolation through graphene flake network under strain. (a) Representation of voltage drop at fixed current in a graphene film at different levels of strain. (b) Resistance–strain diagram for different graphene flake number density  $n$ . (inset) Gauge factor GF as a function of unstrained resistance  $R_0$ .

fixed current increases as the device is strained, in agreement with our experimental observations.

Upon straining, neighboring flakes can lose their contact, and the breakage of percolation pathways occurs. The breakage of a conduction pathway represents a singularity in the resistance–strain behavior, and thus the sensitivity, that is, the derivative of the resistance–strain function, is large. This effect becomes important as the number of percolation pathways is decreased due to the reduction of parallel conduction. Figure 4b quantifies how the morphology of the graphene film affects the sensitivity of the modeled strain gauge. It is shown that devices with a lower flake number density  $n$  exhibit a larger slope in the resistance–strain diagram. The extracted Gauge factors for devices with varying  $n$  are proportional to their initial resistance as shown in the inset of Figure 4b. This behavior is in good qualitative agreement with our experimental observation, but the model underestimates the measured gauge factor. The discrepancy is likely due to simplifying assumptions of the model such as considering a uniform size distribution for the graphene flakes and neglecting clustering of flakes that may occur during the solvent evaporation in the deposition process.

The upper limit of the achievable gauge factor for the described strain gauge class can be estimated from the described geometrical model when considering that maximum sensitivity is achieved at breakage of the last conduction pathway. The expected singular decrease in current vs displacement ( $d$ ) upon breakage would be broadened by the occurring tunneling current between the flakes which scales as  $\exp(-\alpha d(\Delta E)^{0.5})$ . Here  $d$  is the separation between adjacent flakes,  $\Delta E$  is the tunneling barrier height, and  $\alpha$  is a geometry-dependent constant. Based on experimental data for  $\alpha$  from microfabricated tunneling break junctions<sup>17</sup> the ultimate sensitivity achievable with a single flake–flake junction for 10 nm displacement can be estimated to be  $>10^8$  which is several orders of magnitude larger than existing strain gauges and shows the potential of the presented device structure for extremely high sensitivity strain measurements.

The described working principle is not limited to graphene devices but is expected to apply to thin films of overlapping flakes of any material. Since the sensitivity of the device is determined by the morphology of the film, high gauge factors can be expected for devices composed of materials without a piezoresistive effect, such as metal flakes. Furthermore, the described working principle could be combined with other

strain sensing mechanisms, that is, piezoresistivity, to achieve even higher sensitivities.

The use of graphene in this novel type of strain gauge, however, has several advantages. First, the weak out-of-plane bonding of graphene permits the flakes which comprise the film to slide over each other easily, decreasing the bending and buckling which would result in a degrading performance with time. Second, the atomic thickness of graphene allows the flakes to conform to the substrate morphology which makes the application of strain gauges on complex nonplanar surfaces possible. Finally, the transparency of the produced graphene strain gauges offers new fields of application such as touch screens or glass break detectors.

To demonstrate these capabilities, graphene thin films were deposited on a commercial light bulb (Figure 5a). This structure represents several challenges for traditional strain gauges as it is transparent, has convex and concave surface regions, and only exhibits a low deformability before failure. Contact to the graphene film was made through solder points deposited directly on the glass surface. The high transparency of the deposited graphene film and its ability to conform to this surface without wrinkles permits the almost invisible integration of the sensor. Figure 5b shows the change of resistance as a point load of 25 N is applied to the top of the glass bulb. From finite element modeling the total displacement of the glass surface is expected to be in the order of a few micrometer at the position of the strain gauge (see inset of Figure 5b). The observed slow response is due to the gradual application of pressure on the light bulb to avoid fracture. The large resistance change of approximately 6% in response to this small deformation demonstrates the successful operation of the strain gauge under these challenging conditions. This example highlights the potential of using graphene films as strain sensors on existing and complex structures which opens up commercially important applications in structural monitoring and load testing.

**Conclusion.** In summary, we report on a new type of strain gauge based on thin films of overlapping flakes that presents a promising alternative to conventional gauges combining high, tunable gauge factors with low cost production and easy scalability. The utilized spray coating process has proven to be a suitable deposition method enabling a cheap, controlled, patternable film deposition which is compatible with a wide variety of substrates and even allows for deposition on curved surfaces. The morphology-dependent resistance was found to

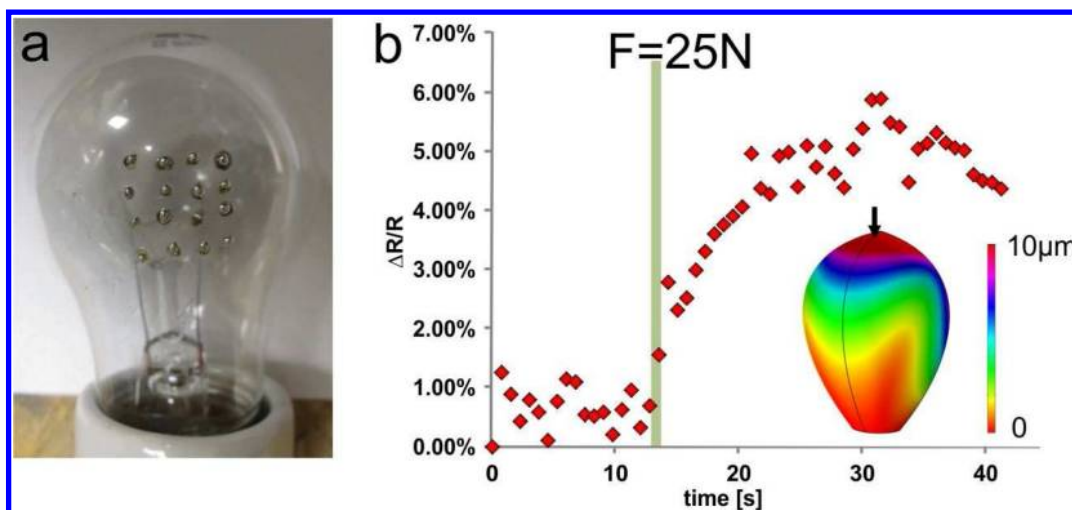


**Figure 5.** Application of graphene strain gauge to complex surface. (a) Photograph of graphene film deposited on light bulb, (b) measurement of electrical response under 25 N point load. (inset) Finite element simulation of total displacement under loading conditions.

correlate closely with the gauge factor which can thus be tuned and has been shown to exceed 150. A model to explain the phenomenon of the tunable sensitivity based on the strain dependent change of flake overlap was verified. Direct deposition of transparent strain gauges on existing structures has large potential for both existing and novel applications in the field of force and deformation sensing.

### ■ ASSOCIATED CONTENT

#### 📄 Supporting Information

Materials synthesis, thin film deposition, Raman analysis, and measurement setups used. This material is available free of charge via the Internet at <http://pubs.acs.org>.

### ■ AUTHOR INFORMATION

#### Corresponding Author

\*E-mail: [mario@mail.ncku.edu.tw](mailto:mario@mail.ncku.edu.tw)

#### Notes

The authors declare no competing financial interest.

### ■ ACKNOWLEDGMENTS

This work is partially supported by Graphene Approaches to Terahertz Electronics (GATE)—MURI grant N00014-09-1-1063 and MIT/Army Institute for Soldier Nanotechnologies (ISN) and the Army Research Laboratory.

### ■ REFERENCES

- (1) *World Stress/Strain Measurement Equipment Markets*; Frost & Sullivan Research Service: Mountain View, CA, 2007.
- (2) Bao, M.-H. *Micro Mechanical Transducers - Pressure Sensors, Accelerometers and Gyroscopes*; Elsevier: New York, 2000; p 392.
- (3) Beeby, S. *Mems Mechanical Sensors*; Artech House: Boston, 2004.
- (4) Geim, A. K.; Novoselov, K. S. *Nat. Mater.* **2007**, *6* (3), 183–191.
- (5) Meric, I.; Han, M. Y.; Young, A. F.; Ozyilmaz, B.; Kim, P.; Shepard, K. L. *Nat. Nano* **2008**, *3* (11), 654–659.
- (6) Balandin, A. A.; Ghosh, S.; Bao, W. Z.; Calizo, I.; Teweldebrhan, D.; Miao, F.; Lau, C. N. *Nano Lett.* **2008**, *8* (3), 902–907.
- (7) Hill, E. W.; Vijayaraghavan, A.; Novoselov, K. *IEEE Sens. J.* **2011**, *11* (12), 3161–3170.
- (8) Wang, Y.; Yang, R.; Shi, Z. W.; Zhang, L. C.; Shi, D. X.; Wang, E.; Zhang, G. Y. *ACS Nano* **2011**, *5* (5), 3645–3650.
- (9) Lee, Y.; Bae, S.; Jang, H.; Jang, S.; Zhu, S. E.; Sim, S. H.; Song, Y. I.; Hong, B. H.; Ahn, J. H. *Nano Lett.* **2010**, *10* (2), 490–493.

(10) Eswaraiah, V.; Balasubramaniam, K.; Ramaprabhu, S. *J. Mater. Chem.* **2011**, *21* (34), 12626–12628.

(11) Zhao, J.; He, C.; Yang, R.; Shi, Z.; Cheng, M.; Yang, W.; Xie, G.; Wang, D.; Shi, D.; Zhang, G. *Appl. Phys. Lett.* **2012**, *101* (6), 063112–5.

(12) Xin, G.; Hwang, W.; Kim, N.; Cho, S. M.; Chae, H. *Nanotechnology* **2010**, *21* (40), 405201.

(13) Zhang, X. Y.; Coleman, A. C.; Katsonis, N.; Browne, W. R.; van Wees, B. J.; Feringa, B. L. *Chem. Commun.* **2010**, *46* (40), 7539–7541.

(14) Hicks, J.; Behnam, A.; Ural, A. *Appl. Phys. Lett.* **2009**, *95* (21), 213103–213107.

(15) Yu, T.; Ni, Z. H.; Du, C. L.; You, Y. M.; Wang, Y. Y.; Shen, Z. X. *J. Phys. Chem. C* **2008**, *112* (33), 12602–12605.

(16) Mohiuddin, T. M. G.; Lombardo, A.; Nair, R. R.; Bonetti, A.; Savini, G.; Jalil, R.; Bonini, N.; Basko, D. M.; Galotiss, C.; Marzari, N.; Novoselov, K. S.; Geim, A. K.; Ferrari, A. C. *Phys. Rev. B* **2009**, *79* (20), 205433–205441.

(17) Zhou, C.; Muller, C. J.; Deshpande, M. R.; Sleight, J. W.; Reed, M. A. *Appl. Phys. Lett.* **1995**, *67* (8), 1160–1162.